

Tween 80–Sodium Deoxycholate Mixed Micelles: Structural Characterization and Application in Doxorubicin Delivery

Jayita Bhattacharjee,[†] Gunjan Verma,[†] V. K. Aswal,[‡] Abhijit A. Date,[§]
Mangal S. Nagarsenker,[§] and P. A. Hassan^{*,†}

Chemistry Division, Solid State Physics Division, Bhabha Atomic Research Centre, Mumbai-400 085, India,
and Department of Pharmaceutics, Bombay College of Pharmacy, Kalina, Santacruz (East),
Mumbai-400098, India

Received: August 30, 2010; Revised Manuscript Received: October 27, 2010

The objective of the present investigation is to develop and characterize anionic mixed micelles of two biocompatible surfactants, Tween 80 (T-80) and sodium deoxycholate (NaDC), and evaluate their potential in the delivery of doxorubicin hydrochloride (DOX), a cationic anticancer drug. The mixed micelles were characterized for their microstructure, intermicellar interactions, and doxorubicin binding ability by dynamic light scattering, small angle neutron scattering (SANS), viscosity, and optical absorption measurements. Salt-induced growth of the mixed micelles at different compositions suggests that both electrostatic interaction of the anionic bile salts and steric repulsion of the ethylene oxide groups in nonionic components are affected by the presence of electrolytes. Addition of bile salt molecules to T-80 micelles suppresses the salt-induced growth of nonionic T-80 micelles. SANS studies indicate that bile salt micelles are prolate ellipsoidal in shape, and the addition of T-80 transforms them toward a spherical shape. The anionic bile salt can successfully bind to the cationic drug doxorubicin. The in vitro cytotoxicity studies in various cancer cell lines revealed that DOX-loaded micelles have greater in vitro anticancer activity as compared to DOX solution, indicating their potential in pharmaceutical applications.

Introduction

Mixed micelles have been employed in the pharmaceutical arena for solubilization of various hydrophobic drugs for the past two decades. The application of mixed micelles for improving therapeutic efficacy of various drugs has been established for different routes of administration, viz., parenteral,¹ oral,² and dermal routes.³ Mixed micelles have been particularly employed for parenteral delivery of hydrophobic drugs. For example, Valium MM and Konakion MM are two mixed-micelle-based formulations currently available in the pharmaceutical market. Mixed micelles usually have diameters lesser than 60 nm, which prevents their uptake by the reticuloendothelial system (RES), increases their in vivo circulation, and facilitates their extravasation in sites with leaky vasculature such as tumors.⁴ However, most of the investigations described in pharmaceutical research employ phospholipids and bile salts for the fabrication of mixed micelles. Furthermore, the method of fabrication of phospholipid–bile salt mixed micelles involves use of organic solvents such as chloroform and methanol, which are required for solubilization of phospholipids.⁵ Hence, there is need to develop alternative mixed micelle formulations using components with good pharmaceutical acceptability.

Polysorbate-80 or Tween-80 (polyoxyethylene-20-sorbitan monooleate; T-80) is a biocompatible nonionic surfactant that is widely used as a solubilizer in pharmaceutical industry. T-80 is one of the widely used excipients in pharmaceutical industry for various applications and is approved by the U.S. Food and

Drug Administration for use in injectable, oral, and topical products.⁶ Furthermore, T-80 has the ability to increase the permeability of various drugs across biological membranes.⁷ Its potential to inhibit P-glycoprotein (P-gp)-mediated efflux of various P-gp substrates has been established.⁸ Similarly, bile salts are physiologically relevant, and biocompatible molecules derived from cholesterol and can undergo aggregation in aqueous solution.⁹ The mechanism of bile salt association is different from that of conventional surfactants, mainly due to its structural difference. Sodium deoxycholate (NaDC) is a water-soluble bile salt having good acceptability for pharmaceutical products. In fact, NaDC is used in the mixed micellar formulation of Amphotericin B (antifungal agent), which is currently marketed as Fungizone.¹⁰ NaDC is known to enhance the permeation of various drugs across biological membranes.¹¹ Thus, it is envisaged that mixed micelles based on T-80 and NaDC would have good acceptability in pharmaceutical research for drug delivery. Furthermore, the preparation of T-80–NaDC mixed micelles would be very easy as both components are water-soluble.

The micellization behavior of NaDC in the presence of T-80 has been reported using surface tension and fluorescence measurements.¹² However, to the best of our knowledge, there is no report on microstructure elucidation or drug delivery applications of mixed micelles composed of T-80 and NaDC. Hence, the main objectives of this investigation are to elucidate the microstructure of the T-80–NaDC mixed micelles and to evaluate the ability of these micelles to incorporate ionic drugs. The ionic drug chosen for this investigation was doxorubicin hydrochloride (DOX), a water-soluble anticancer agent. The ionic mixed micelles of T-80–NaDC presented in the investigation are expected to encapsulate DOX via noncovalent electrostatic interaction while eliminating complex chemical synthesis.

* To whom correspondence should be addressed. Tel: + 91-22 25595099.
Fax: + 91-22 25505151. E-mail: hassan@barc.gov.in.

[†] Chemistry Division, Bhabha Atomic Research Centre.

[‡] Solid State Physics Division, Bhabha Atomic Research Centre.

[§] Bombay College of Pharmacy.

The DOX-loaded mixed micelles were evaluated for in vitro cytotoxicity against various cancer cell lines to establish their potential in improving the delivery of DOX.

Experimental Section

Chemicals. T-80, NaDC, and sodium chloride (NaCl) salt were obtained from S.D. Fine Chemicals. DOX was obtained from Sun Pharmaceuticals, Baroda. All chemicals were used as such without further purification. Stock solutions of T-80 and NaDC were prepared in deionized water and mixed in varying ratios.

Dynamic Light Scattering. Dynamic light scattering (DLS) measurements were performed using a Malvern 4800 Autosizer employing a 7132 digital correlator. The light source was an argon ion laser operated at 514.5 nm with a maximum power output of 2 W. The correlation functions were analyzed by the method of cumulants.

Viscosity. Viscosity measurements were carried out using an Ubbelohde suspended level capillary viscometer. The viscometer was suspended vertically in a thermostat at a temperature of 45 ± 0.1 °C. The viscometer was cleaned and dried before each measurement. The flow time for constant volume of solution through the capillary was measured with a calibrated stopwatch.

Small Angle Neutron Scattering. Small angle neutron scattering (SANS) experiments were carried out using the SANS diffractometer at the Dhruva Reactor, Bhabha Atomic Research Centre, Trombay, India. The diffractometer makes use of a beryllium oxide-filtered beam of mean wavelength (λ) 5.2 Å. The angular distribution of the scattered neutrons was recorded using a one-dimensional position-sensitive detector (PSD). The accessible wave vector transfer [$Q = (4\pi \sin \theta)/\lambda$, where 2θ is the scattering angle] range of the diffractometer is 0.017–0.35 Å⁻¹. The PSD allows simultaneous recording of data over the full Q range. The samples were held in a quartz sample holder of 0.5 cm thickness. In all measurements, the temperature was kept fixed at 45 °C. The measured SANS data were corrected and normalized to a cross sectional unit, using standard procedures. SANS studies were carried out on a mixed micellar solution of T-80 and NaDC at different mole fractions.

In Vitro Cytotoxicity Studies. The cytotoxicity of free DOX, DOX-loaded T-80–NaDC mixed micelles, and blank T-80–NaDC mixed micelles was tested against various human cancer cell lines, viz., human colon cancer cell line (Colo205), human oral cancer cell line (Gurav), and human cervix cancer cell line (ME180). Various human cancer cell lines were cultured in RPMI-1640 medium supplemented with fetal bovine serum (FBS, 10%) and 2 mM L-glutamine and maintained at 37 °C in a CO₂ incubator in an atmosphere of 5% CO₂ in Nunc Tissue culture flasks. The cells were seeded in 96-well microtiter-plates (at a concentration of 1×10^4 cells/well) and incubated for 24 h to ensure adequate growth before determination of cell growth inhibition. After 24 h from seeding, sterile test compounds (DOX, DOX + micelles, and blank micelles) were added in triplicate in wells at different concentrations (10^{-4} to 10^{-7} M). Cytotoxicity caused by the test compounds was evaluated using the sulforhodamine B (SRB) assay protocol. Briefly, the cells were further incubated at 37 °C in a CO₂ incubator for 48 h. These nonadherent cell cultures were then fixed in situ by slow addition of cold 30% trichloroacetic acid (TCA). The plate was then kept at 4 °C for 1 h. The supernatant was discarded, and all the wells were washed five times with water. Plates were then air-dried. SRB solution (0.4% w/v in 1% acetic acid) was added to each of the wells, and the plate was kept at room temperature for 20 min. The unbound dye was removed by

washing five times with 1% acetic acid. The plate was flicked several times to remove traces of moisture, followed by air-drying. Bound dye was then extracted by addition of 10 mM Tris base (pH 10.5) to each of the wells. Optical density was measured at 540 nm on an ELISA microplate reader. The concentration of test formulations that led to 50% cytotoxicity (LC₅₀) was calculated.

Results and Discussions

T-80–NaDC Mixed Micelles. A mixed micelle comprising T-80 and NaDC offers the advantages of polyoxyethylene stealth to the micelles as well as anionic nature for binding of cationic drugs. First, we investigated the microstructure and nature of intermicellar interaction in mixed micelles of varying composition using light scattering. Both NaDC and T-80 form nearly globular aggregates at concentrations near their critical micelle concentration (CMC). To minimize the effect of intermicellar interaction and consequent decrease in the scattering intensity, initial experiments were carried out in the presence of 0.4 M NaCl. The Kraft point of NaDC is sensitive to electrolyte concentration. It increases with the addition of NaCl and approaches room temperature at about 1.4 M NaCl. DLS measurements were carried out at 45 °C, which is well above the Kraft point of NaDC.

In DLS, the normalized time correlation function of the scattered intensity, $g^{(2)}(\tau)$ is expressed as

$$g^{(2)}(\tau) = \langle I(o)I(\tau) \rangle / \langle I \rangle^2 \quad (1)$$

For photo counts obeying Gaussian statistics, $g^{(2)}(\tau)$ is related to the first-order correlation function of the electric field $g^{(1)}(\tau)$ by the Siegert relationship

$$g^{(2)}(\tau) = a + b|g^{(1)}(\tau)|^2 \quad (2)$$

where a is the baseline and b is an adjustable parameter dependent on the scattering geometry and independent of τ . For a suspension of monodisperse, spherical particles undergoing Brownian diffusion, the autocorrelation function decays exponentially and is given as

$$g^{(1)}(\tau) = \exp(-Dq^2\tau) \quad (3)$$

where D is the translational diffusion coefficient. The hydrodynamic radius R_h can be obtained from the translational diffusion coefficient using the Stokes–Einstein relationship

$$D = kT/(6\pi\eta R_h) \quad (4)$$

where k is the Boltzmann constant, η is the solvent viscosity, and T is the absolute temperature.

Figure 1 shows the variation in the diffusion coefficient and apparent hydrodynamic radius of the NaDC–T-80 mixed micelles (total concentration of 100 mM) as a function of the mole fraction of T-80. The hydrodynamic radius of NaDC-rich micelles is about 2.5 ± 0.4 nm, while that of T-80 is 6.1 ± 0.3 nm. The larger hydrodynamic radius of T-80 micelles as compared to NaDC is consistent with the long polyoxyethylene-based head groups of T-80. Lafitte et al. reported a hydrodynamic radius of 5.7 nm for 5% T-80 micelles in water.¹³ The diffusion coefficient measured by DLS rests on the assumption

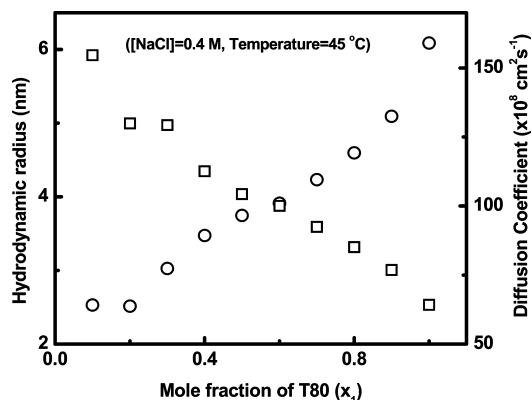


Figure 1. Variation of apparent hydrodynamic radius (R_h) and diffusion coefficient (D_a) of T-80–NaDC mixed micelles with varying mole fraction of T-80 (total surfactant concentration 0.1 M) in the presence of 0.4 M NaCl.

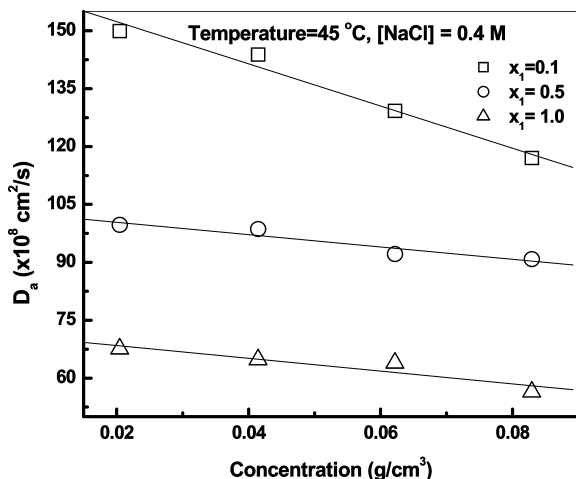


Figure 2. Variation of the apparent diffusion coefficient of T-80–NaDC mixed micelles (D_a) with total surfactant concentration, at different compositions.

that there is negligible interparticle interaction between the diffusing particles. To identify the nature of interparticle interaction in mixed micelles, concentration dependences of the diffusivities are measured at three different mole fractions. When intermicellar interactions are present, the apparent diffusion D_a can be related to the diffusion virial coefficient, k_D by the relation

$$D_a = D_0[1 + k_D \cdot C] \quad (5)$$

where D_0 is the infinite dilution diffusion coefficient, and C is the concentration (in g/mL). The variations of D_a with surfactant concentration at three different mole fractions are depicted in Figure 2. The solid lines in Figure 2 represent linear fit to the measured data using eq 5. From the slope and intercept of eq 5, D_0 and k_D can be obtained. The best fit values of k_D , D_0 , and the corresponding R_h as calculated from D_0 are summarized in Table 1. The slope of D_a versus C is negative, indicating negative values of k_D at all three mole fractions investigated. The parameter k_D is related to the thermodynamic second virial coefficient by the relation

$$k_D = 2A_2M_w - k_f - 2v \quad (6)$$

where k_f is the friction coefficient, M_w is the micelle molecular weight, and v is the specific volume of the micelles in the

TABLE 1: Best Fit Values of k_D , D_0 , and the Corresponding R_h as Calculated for Different Mole Fractions of T-80

mole fraction of T-80	D_0	k_D (cm ³ /g)	R_h (nm)
0.1	163×10^{-8}	−544	2.4
0.5	103×10^{-8}	−159	3.75
1.0	71×10^{-8}	−165	5.4

solution. If we accept the approximation that k_f and v are concentration independent, the value of k_D will reflect the changes in the virial coefficient A_2 . For salt free ionic micelles, where repulsive intermicellar interactions are present, the sign of k_D should be positive, unless the micelles undergo a structural change with concentration. The negative value of k_D observed even for NaDC-rich micelles implies a substantial growth of the micelles with increase in concentration. This is consistent with the DLS studies on dihydroxy bile salt micelles. Janich et al. determined the concentration dependence of the diffusion coefficient and molar mass of sodium glycodeoxycholate micelles in the presence of electrolytes using light scattering.¹⁴ It is noted that both molar mass and diffusion coefficient vary monotonically with increasing bile salt concentration. Increasing the ionic strength of the solution by adding NaCl, the sign of k_D changes from positive to negative. In the low salt regime, i.e., $[NaCl] < 0.2$ M, the slopes are positive with a linear variation in the apparent diffusion coefficient. At higher salt content, the slopes are negative, an observation that is explained in terms of the growth of the micelles with increase in surfactant concentration. Such inversion in the sign of k_D is reported for other ionic micelles, too.^{15–18} The value of k_D depends on micellar structural changes as well as interparticle interactions. These two factors affect the apparent diffusion coefficient in opposite ways. The magnitude and sign of the measured k_D depends on which of the two factors dominate. Considering the anionic nature of NaDC micelles, the repulsive Coulombic interaction between the micelles should lead to positive k_D . The observed negative values of k_D suggest that the changes in the apparent diffusion coefficient is dominated by salt-induced micellar growth. If attention is paid to the magnitude of k_D values at different compositions, it is noted that the interaction parameter at the intermediate composition is lower than that of pure components. Considering the electrostatic effects alone, we expect that the interaction parameter is the lowest for pure nonionic micelles. However, the above observation reveals that electrolytes such as NaCl can induce growth of nonionic-rich micelles as well. This can be confirmed from the variation in the diffusion coefficient of the micelles as a function of electrolyte concentration.

To understand salt-induced changes in the structure of mixed micelles, DLS measurements were performed at different concentrations of salt, from 0.4 to 1.4 M at 45 °C (Figure 3). At all mole fractions, the diffusion coefficient of the micelles decreases monotonically with salt concentration. The observed changes in D_a with the addition of electrolyte arise from the change in the size of the micelles. A pronounced decrease in apparent diffusion coefficient is observed in NaDC-rich micelles. Moreover, the D_a of NaDC-rich micelles show a nonlinear behavior at high salt concentrations. The slope of the plot, at low ionic strength, is the highest for NaDC-rich micelles. This is consistent with the enhanced Coulombic repulsion of charged head groups in NaDC micelles. Addition of salts screens the charge on NaDC molecules and promotes micellar growth. This complies with the magnitude of the diffusion virial coefficient reported in Table 1. In the presence of 1.4 M NaCl, the apparent hydrodynamic radii of the mixed micelles show a minimum at

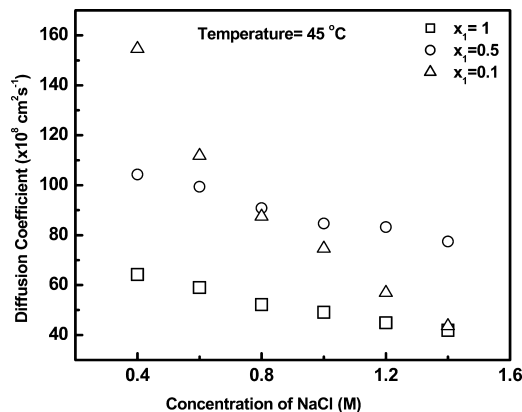


Figure 3. Variation of micelle diffusion coefficient (D_s) with NaCl concentration, at different mole fractions (total surfactant concentration is 0.1 M).

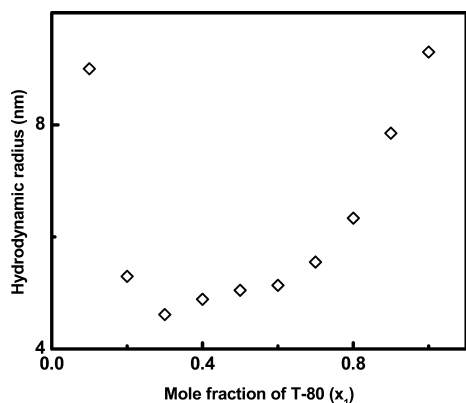


Figure 4. Variation of apparent hydrodynamic radius (R_h) of T-80–NaDC mixed micelles (total surfactant concentration 0.1 M) at 1.4 M NaCl and at 45 °C.

intermediate mole fraction (Figure 4). This suggests that both nonionic and anionic rich micelles are susceptible to electrolyte-induced micellar growth.

The above observations highlight the relative importance of the electrostatic and steric contributions of the head groups to the free energy of micellization. Although added electrolytes can affect the structure of nonionic micelles, its effects are expected to be relatively small for pure T-80. However, in the present study, the observed variation in the hydrodynamic radius suggests a pronounced growth of nonionic micelles. Similar results have been reported in a nonionic–anionic mixture containing hexaethylene glycol monododecyl ether (C_{12}E_6) and sodium dodecyl sulfate.¹⁹ Penfold et al. have shown from some recent SANS studies that micelles rich in C_{12}E_6 compositions exhibit pronounced micellar growth with the addition of electrolyte. From applications of the molecular thermodynamic theory of Shiloach and Blankshtein,²⁰ it is argued that this is due to the subtle balance between the steric and electrostatic contributions to the free energy of micellization. The predominant factor to the free energy of micellization is the large negative contribution from the transfer of the hydrocarbon chain from the aqueous environment to the hydrocarbon micellar core. This is typically on the order of 18–19 kJ.²¹ The pronounced growth of T-80 micelles in the presence of electrolyte implies that there is an electrolyte-dependent contribution to the steric free energy of ethylene oxide groups. Based on quasielastic light scattering (QELS) studies, Phillies et al. concluded that the aggregation number and hydration of nonionic Triton X-100 micelles can be altered by changing the concentration of

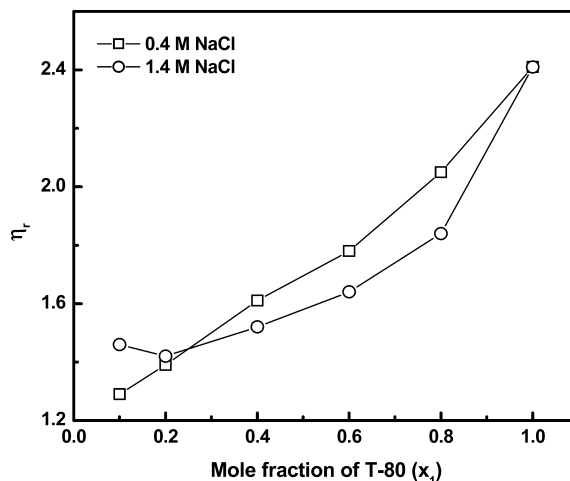


Figure 5. Variation of relative viscosity of mixed micelles with mole fraction of T-80 at 45 °C and at different NaCl concentrations (0.4 and 1.4 M).

background electrolyte.²² Electrical interactions of the background electrolyte with the dielectric constant gradient at the micelle surface or with the solvent affect the aggregation behavior. This is akin to the reduction of the nonionic clouding temperature with the addition of electrolytes. Carale et al.²³ considered the effect of different electrolytes on intramolecular interactions and on micellization of polyethylene oxide-based nonionic surfactants. It is concluded that the most pronounced effect was on the solubility of the alkyl chain, primarily by decreasing the solubility of the alkyl moieties with the addition of electrolytes. With the addition of an ionic component, electrostatic repulsion of the head groups will depress this effect. Tatiana et al.²⁴ attribute the sensitivity of the composition induced changes in micellar size with added electrolyte to changes in the enthalpy of micellization due to partial dehydration of the ethylene oxide headgroups. The addition of an ionic component increases the headgroup repulsion, resulting in an increased hydration due to a greater exposure of the headgroups to the solvent phase, and hence minimizing the effects of dehydration. This is qualitatively consistent with our observations for NaDC/T-80 mixed micelles.

Viscosity measurements were performed as an independent check of the above observed micellar structural changes. Figure 5 shows composition-dependent variations in the relative viscosity of mixed micelles at 45 °C and at different NaCl concentrations (0.4 and 1.4 M). The relative viscosity of a dilute micellar solution is given by

$$\eta_r = 1 + \nu\phi + k_1(\nu\phi)^2 \quad (7)$$

where ν is a factor that depends on the geometry of the micelles and ϕ is the volume fraction of the micelles. The quadratic term accounts for hydrodynamic interactions and the constant k_1 is a measure of hydrodynamic interactions. For a dilute solution of rigid noninteracting spheres, the quadratic term can be neglected, and ν equals 2.5 regardless of the size of the sphere, according to the Einstein equation.²⁵ From the known dry volume fraction of micelles, the shape factor ν can be computed from the relative viscosity data. At low NaCl concentration, the relative viscosity varies linearly with the composition of the micelles. At all compositions, the shape factor ν is found to be higher than 2.5, the expected value for hard sphere suspensions, and the effect is more pronounced in the nonionic rich region. This could arise

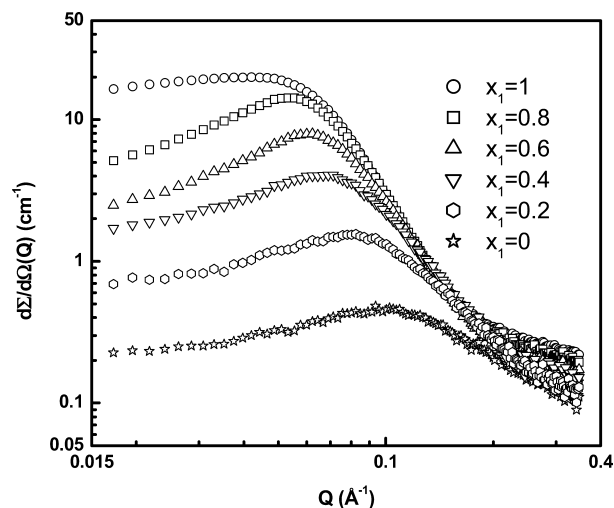


Figure 6. SANS spectra for T-80–NaDC mixed micelles (total concentration of surfactants 0.1 M) at different mole fraction of T-80 and at 45 °C.

from the changes in the volume fraction of the micelles due to hydration of the polyoxyethylene chain. At 1.4 M NaCl, the relative viscosity decreases initially and then increases with increase in mole fraction. This is due to the pronounced growth of NaDC-rich micelles and T-80 micelles in the presence of 1.4 M NaCl, while a moderate growth is observed at intermediate mole fraction. This result is consistent with the hydrodynamic radius measured by DLS.

Micelle Characterization by SANS. Figure 6 shows the SANS data from NaDC/T-80 mixed micelles in D₂O at 45 °C. The evolution of the SANS spectra at different solution compositions indicate the formation of small globular micelles. The data at all compositions show a correlation peak indicating the occurrence of strong intermicellar interaction. It is observed that, with increasing mole fraction of T-80, the correlation peak shifts to lower Q value indicating an increase in the size of the micelles.

At low volume fractions, the NaDC micelles are best described using a prolate ellipsoidal structure interacting through a screened Coulomb potential. Thus, this model is used for the analysis of the SANS data. The coherent differential scattering cross section $d\Sigma/d\Omega$ can be expressed as²⁶

$$\frac{d\Sigma}{d\Omega} = n(\rho_m - \rho_s)^2 V^2 [\langle F(Q)^2 \rangle + \langle F(Q) \rangle^2 (S(Q) - 1)] + B \quad (8)$$

where n denotes the number density of the micelles, ρ_m and ρ_s are the scattering length densities of the micelle and the solvent, respectively, and V is the volume of the micelle. $F(Q)$ is the single particle form factor for prolate ellipsoids, and $S(Q)$ is the interparticle structure factor. B is a constant term that represents the incoherent scattering background. For $S(Q)$ calculation, prolate ellipsoidal micelles are assumed to be rigid equivalent spheres of diameter $\sigma = 2(ab^2)^{1/3}$ interacting through a screened Coulomb potential. The dimensions of the micelle, aggregation number, and fractional charge have been determined from the model fitting of the SANS data. The semimajor axis (a), semiminor axis (b), and the fractional charge (α) are the parameters used for analyzing the SANS data. The prolate ellipsoidal model with screened Coulomb interaction in the rescaled mean spherical approximation fits well with the SANS

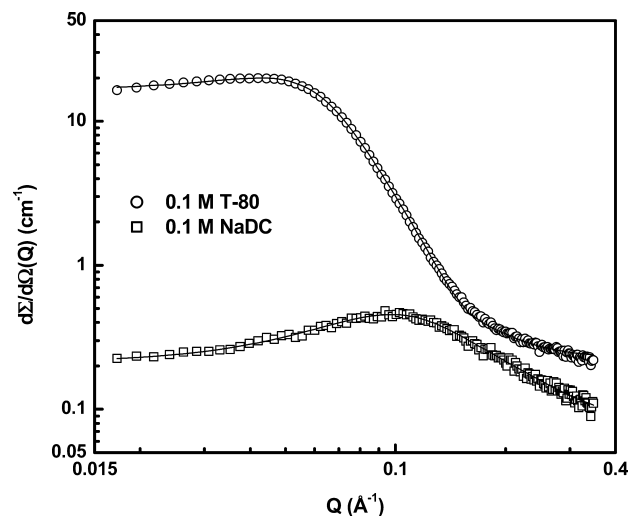


Figure 7. SANS data of 0.1 M NaDC and T-80 micelles along with model fits to the spectra using appropriate models discussed in the text.

TABLE 2: Micellar Parameters Obtained from SANS Analysis of 0.1 M NaDC Micelles Using Prolate Ellipsoidal Structure and Rescaled Mean Spherical Approximation (RMSA) Closure Relation

semimajor axis (a) (nm)	semiminor axis ($b = c$) (nm)	effective radius (ab^2) ^{1/3} (nm)	fractional charge	aggregation number
3.29	0.88	1.37	0.47	15

TABLE 3: Micellar Parameters Obtained from SANS Analysis of 0.1 M T-80 Micelles Using Percus–Yevick Approximation

core radius R_C (nm)	polydispersity	hard sphere radius R_{HS} (nm)	volume fraction	aggregation number
2.56	0.25	4.69	0.11	179

spectra of pure NaDC micelles (Figure 7). The values of fitted parameters namely, semimajor axis, semiminor axis, aggregation number, and fractional charge on the micelles are given in Table 2. The above model is not applicable to the SANS data of pure T-80 micelles. This is due to the presence of bulky polyoxyethylene chains on the micelle surface and zero surface charge of the nonionic micelles. These micelles are best described by polydisperse core–shell spheres interacting through hard sphere repulsion. Thus, the interparticle structure factor $S(Q)$ for T-80 micelles was estimated by the analytical solution of the Ornstein–Zernike equation with the Percus–Yevick approximation, employing hard sphere interaction (Figure 7). The refined values of the micelle parameters are given in Table 3, and it suggests that a core–shell sphere is an appropriate model for T-80 micelles. The dimension of core and shell are consistent with the recent results obtained by inverse Fourier transform (IFT) analysis of the small angle X-ray scattering (SAXS) data.²⁷

The inadequacy of a single model to describe the structure of both T-80 and NaDC micelles restrict model fitting of the SANS data of mixed micelles at intermediate mole fractions. This is due to the complexity of the calculation of $S(Q)$ where the charged head groups of NaDC gets hidden by the large hydrated head groups of T-80. However, the scattering patterns, over the entire composition range, remain consistent with significant intermicellar interaction. The peak in the scattering pattern, associated with intermicellar interaction, shifts systematically to lower Q values. Without going into the details of micelle shape, one can calculate the mean aggregation number from the peak position (Q_m), assuming a simple cubic (SC) or

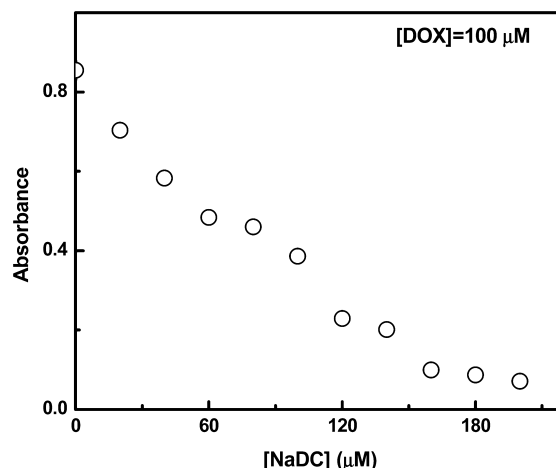
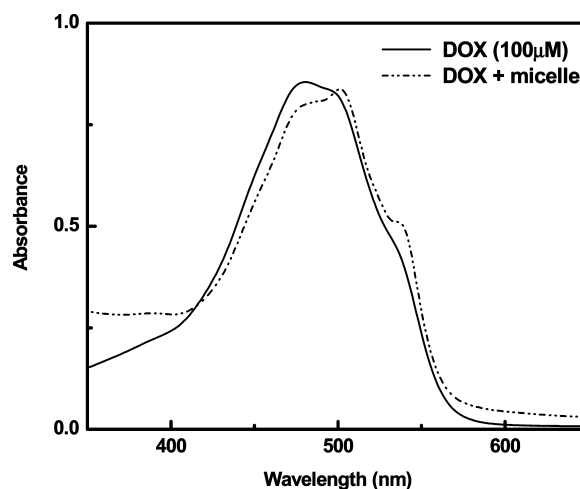
TABLE 4: Micellar Parameters of NaDC and T-80 Mixed Micelles As Derived from the Peak Position of SANS Data

T-80 mole fraction (x_1)	peak position Q_p (\AA^{-1})	aggregation number (FCC model)	aggregation number (SC model)	effective micellar radius (SC model) R (nm)
1.0	0.04204	261	201	4.71
0.8	0.05329	128	99	3.54
0.6	0.06003	90	69	2.96
0.4	0.06677	65	50	2.48
0.2	0.08247	35	27	1.85
0	0.10262	18	14	1.32

face-centered cubic (FCC) packing of the micelles. The relevant equations that relate Q_m and the aggregation number can be found elsewhere.²⁸ The aggregation numbers calculated using the above approach, assuming SC and FCC packing, are summarized in Table 4. It may be noted that the aggregation numbers of pure T-80 and NaDC micelles calculated from the SC approximation are closer to the values obtained from model fitting. Thus, the effective radius of the mixed micelles at different mole fractions were evaluated from the SC packing model and are included in Table 4.

The overall analysis of SANS data at different compositions of NaDC and T-80 suggests an increase in the aggregation number of the micelles with increasing mole fraction of T-80. The results obtained from SANS experiments are in accordance with the one obtained from DLS studies. The slightly higher values of apparent radius obtained by DLS as compared to the one obtained by SANS analysis arises from the hydration of the micelles. The micellar structure is consistent with simple packing considerations, which imply that T-80 molecules with their relatively larger headgroup volume would promote highly curved interfaces. On the other hand, the molecular structure of NaDC is conducive for formation of prolate ellipsoidal micelles.

Binding of DOX to Mixed Micelles. It is of primary importance to assess the drug binding ability of these micelles through electrostatic complexation of cationic drugs, as this may provide a basis to design novel drug delivery vehicles. DOX is chosen as a model cationic drug for this purpose. DOX is an anthracycline antibiotic, which are considered essential components of first-line chemotherapy in the treatment of a variety of solid and hematopoietic tumors.²⁹ However, the use of DOX is associated with serious dose-limiting toxicities, including cardiotoxicity and nephrotoxicity. In order to reduce the side effects associated with DOX, various colloidal carriers such as liposomes, nanoparticles, and polymeric micelles have been investigated. In particular, polyethylene glycol (PEG)-coated stealth liposomes have been widely explored for improving efficacy and reducing side effects such as cardiotoxicity.²⁹ Recently, block copolymer micelles comprising anionic functionalities such as lactic acid or acrylic acid have also been developed for electrostatic binding of DOX.^{30–33} This protocol involves the chemical modification of the block copolymer with anionic moieties to achieve electrostatic binding with cationic DOX. Such an electrostatic binding approach can be extended to the present mixed micellar system for the complexation of doxorubicin. To understand the ability of DOX to complex with NaDC, the partitioning of DOX between water and chloroform was monitored. The effect of the DOX-to-NaDC ratio on the extraction efficiency of DOX into chloroform was examined from optical absorption measurements. Figure 8 shows variation in the absorbance of the chloroform phase (at 481 nm) as a function of NaDC concentration, for a constant concentration of DOX (0.1 mM).

**Figure 8.** Variation in the absorbance of DOX in the chloroform layer (481 nm) with varying concentrations of NaDC, keeping the concentration of DOX fixed at 100 μM .**Figure 9.** Optical absorption spectra of pure DOX and DOX in T-80–NaDC mixed micelles.

The concentration of DOX in the chloroform layer increases with the NaDC concentration and DOX was extracted almost completely above NaDC concentration of 0.2 mM. This suggests that the addition of NaDC increases the hydrophobicity of DOX through electrostatic complexation and can be partitioned completely into the organic phase. A slight change in the optical absorption spectrum of DOX upon addition of NaDC was observed (Figure 9). The spectrum shows a red shift as well as change in relative intensities at the peak to the shoulder, upon complexation. A similar shift in the optical absorption is observed when DOX is encapsulated in polymer hydrogel nanoparticles³⁴ and in a DOX–aerosol-OT (AOT) complex.³⁵ In the absence of any organic solvents, the DOX–NaDC complex precipitates from the aqueous solution, indicating the formation of an ion-pair complex. This complex can be solubilized by the addition of T-80 through mixed micelle formation. This demonstrates the ability of T-80–NaDC mixed micelles to bind model cationic drugs such as DOX.

Cytotoxicity Studies. Cytotoxicity of T-80–NaDC mixed micelles on three different cancer cell lines were measured in order to identify their biocompatibility for use in pharmaceutical applications. Figure 10 shows the percentage growth of various human cancer cell lines in the presence of 10 $\mu\text{g/mL}$ mixed micelles (5 $\mu\text{g/mL}$ T-80 and 5 $\mu\text{g/mL}$ NaDC) after 48 h of incubation. Nearly 100% survival of the cells in the presence

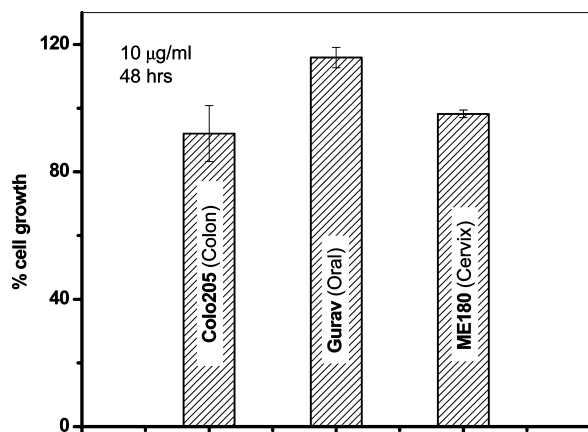


Figure 10. Percentage growth of various human cancer cell lines in the presence of 10 $\mu\text{g/mL}$ blank mixed micelles (without DOX).

of mixed micelles indicate negligible cytotoxicity of the surfactants at concentrations less than 10 $\mu\text{g/mL}$. The cytotoxicities of formulations comprising DOX and mixed micelles were evaluated in comparison to free DOX. The LC_{50} values obtained for the test formulations in different cell lines are expressed in Table 5. It is evident from Table 5 that DOX-loaded mixed micelles showed significantly lower LC_{50} value for all the cell lines as compared to that of plain DOX solution. The LC_{50} values of plain DOX and DOX-loaded micelles are different for various cell lines, which is due to the difference in sensitivity or potency of DOX toward a particular cancer type.

It may be noted that plain DOX and DOX micelles are most potent for human cervix cancer. The DOX-loaded mixed micelles showed 2- to 10-fold lower LC_{50} values as compared to that of plain DOX in various cell lines. This clearly indicates that mixed micelles not only encapsulate the DOX but also significantly improve anticancer activity of DOX in various cancer cell lines. The blank mixed micelles did show signs of cytotoxicity, but at a concentration that is approximately 10-fold higher than used for the fabrication of DOX-loaded mixed micelles (data not shown). Hence, it can be assumed that the enhanced anticancer activity of DOX-loaded micelles is not due to the components of mixed micelles. It is reported in the literature that T-80 has the ability to increase the permeability of the drug across various cell lines such as Caco 2 cells.³⁶ It has been demonstrated that T-80 can increase intracellular uptake of epirubicin, a doxorubicin analogue by increased permeability and by inhibition of P-gp-mediated or multidrug resistance (MDR)-mediated efflux.^{36,37} Hence, the enhanced anticancer activity of the DOX-loaded mixed micelles could be due to increased cellular uptake of the DOX. Recent studies show that polymeric micelles with a PEG shell can be used to enhance the oral uptake of various hydrophobic drugs.³⁸ A model hydrophobic compound vitamin K was encapsulated in PEG containing thermosensitive block copolymer micelles. In vitro studies suggest that vitamin K plasma levels rose significantly upon gastric administration of the drug-loaded micelles in sham operated rats. Addition of certain bile acids such as deoxycholic acid further enhances the absorption of micelle-encapsulated hydrophobic molecules in the gastrointestinal tract.³⁸ The

efficacy of mixed micelles in devising new drug delivery systems has been demonstrated in a classic paper by Lasic.³⁹ Thermodynamically stable large disk-like mixed micelles comprising amphotericin B and a biological lipid demonstrated a significantly improved therapeutic index.

Bile salts demonstrate multiple advantages as drug delivery excipients; they enhance the permeability of certain drugs, increase plasma membrane fluidity, and inhibit MDR associated with epirubicin.^{37,40,41} Thus, the components used for mixed micelles in the present investigation have potential to increase uptake of the drug by cancer cell lines mainly by modulating its permeability and P-gp- and/or MDR-mediated efflux. These are the potential reasons for significant reduction in the LC_{50} value as observed in the case of DOX-loaded micelles. Furthermore, this can be extended to other cationic drugs to form ion-pair complexes with anionic NaDC. The ion-pair complex formation increases the lipophilicity of the DOX, which would in turn increase the uptake of DOX by cancer cells. Similar observation has already been reported for the transport of a natural alkaloid berberine.⁴² On the basis of these observations, we propose that the mixed micelles reported in the present investigation can also be used for improving the cellular uptake and therapeutic efficacy of various other cationic drugs (such as ciprofloxacin hydrochloride) used for diseases other than cancer.

Conclusions

We have studied the microstructure, drug binding ability, and cytotoxicity of mixed micelles comprising two biocompatible ingredients, T-80 and NaDC, using complementary techniques. Stable aggregates are formed at all compositions, and the apparent hydrodynamic diameter of the micelles show almost linear variation with composition, at low electrolyte concentration (0.4 M NaCl). The net intermicellar interaction is found to be repulsive in nature at all compositions, suggesting significant steric repulsion of the hydrated oxyethylene head groups in the nonionic micelles. The sensitivity of these micelles toward salt-induced growth is found to be lowest at intermediate composition. Both electrostatic interaction of the anionic bile salts and steric interaction of the ethylene oxide groups in nonionic component are affected by the presence of electrolytes. The interplay of these two effects leads to a minimum in the apparent dimension of the micelles at equimolar composition, in the presence of 1.4 M NaCl. The salt-induced growth of bile salt-rich micelles arises from the screening of the Coulombic repulsion of the ionic head groups. For nonionic rich micelles, changes in the hydration of the shell and hydrophobicity of the core due to changes in the dielectric constant of the medium are responsible for the salt-induced growth. Addition of bile salt molecules to T-80 micelles suppresses the salt-induced growth of nonionic T-80 micelles. The calculated intrinsic viscosities of the mixed micelles in the absence and presence of electrolyte are consistent with the apparent diameter of the micelles. SANS studies in the absence of any added electrolyte indicates a correlation peak in the spectra at all compositions. Bile salt micelles are prolate ellipsoidal in shape, while T-80 forms polydisperse core-shell micelles. An equimolar mixture

TABLE 5: LC_{50} Values Obtained for the Test Formulations in Different Cell Lines

formulation	LC_{50} (M) human colon cancer cell line - Colo 205	LC_{50} (M) human oral cancer cell line - Gurav	LC_{50} (M) human cervix cancer cell line - ME 180
DOX-loaded mixed micelle	2.63×10^{-6}	2.81×10^{-6}	1.85×10^{-7}
DOX	3.86×10^{-5}	3.45×10^{-5}	2.12×10^{-6}

of NaDC and T-80 forms micelles with the characteristics of both anionic headgroup and polyoxyethylene shell. These are less sensitive to electrolyte concentration as compared to the pure components. The anionic component in the micelle is conducive for binding of cationic drug molecules to the micelle surface, while the polyoxyethylene stealth of the micelle can protect the drug from RES uptake. A model cationic drug, DOX, can be made hydrophobic by complexation with the bile salt and can be further incorporated in the mixed micelle for potential applications. Cytotoxicity studies of DOX-loaded micelles to various human cancer cell lines indicate enhanced drug activity. The present findings on the microstructure and drug binding ability of the mixed micelles have important implications in designing micellar carriers for drug delivery.

Acknowledgment. We thank Dr. A. Juvekar of the Advanced Centre for Treatment Research and Education in Cancer (ACTREC), Mumbai, for assistance in carrying out cytotoxicity studies.

References and Notes

- (1) Sznitowska, M.; Klunder, M.; Placzek, M. *Chem. Pharm. Bull. (Tokyo)* **2008**, *56*, 70–74.
- (2) Mrestani, Y.; Behbood, L.; Härtl, A.; Neubert, R. H. *Eur. J. Pharm. Biopharm.* **2010**, *74*, 219–222.
- (3) Hendradi, E.; Obata, Y.; Isowa, K.; Nagai, T.; Takayama, K. *Biol. Pharm. Bull.* **2003**, *26*, 1739–1743.
- (4) Rupp, C.; Steckel, H.; Müller, B. W. *Int. J. Pharm.* **2010**, *387*, 120–128.
- (5) Hammad, M. A.; Müller, B. W. *Eur. J. Pharm. Biopharm.* **1998**, *46*, 361–367.
- (6) Strickley, R. G. *Pharm. Res.* **2004**, *21*, 201–230.
- (7) Rege, B. D.; Yu, L. X.; Hussain, A. S.; Polli, J. E. *J. Pharm. Sci.* **2001**, *90*, 1776–1786.
- (8) Hugger, E. D.; Novak, B. L.; Burton, P. S.; Audus, K. L.; Borchardt, R. T. A. *J. Pharm. Sci.* **2002**, *91*, 1991–2002.
- (9) Jiang, L.; Wang, K.; Deng, M.; Wang, Y.; Huang, J. *Langmuir* **2008**, *24*, 4600–4606.
- (10) Brajtburg, J.; Bolard, J. *Clin. Microbiol. Rev.* **1996**, *9*, 512–531.
- (11) Sharma, P.; Varma, M. V.; Chawla, H. P.; Panchagnula, R. *Farmaco* **2005**, *60*, 874–883.
- (12) Haque, E. M.; Das, A. R.; Moulik, S. P. *J. Colloid Interface Sci.* **1991**, *217*, 1–7.
- (13) Lafitte, G.; Thuresson, K.; Jarwoll, P.; Nydn, M. *Langmuir* **2007**, *23*, 10933–10939.
- (14) Janich, M.; Lange, J.; Graener, H. *J. Phys. Chem. B* **1998**, *102*, 5957–5962.
- (15) Dorshow, R.; Briggs, J.; Bunton, C. A.; Nicoli, D. F. *J. Phys. Chem.* **1982**, *86*, 2388–2395.
- (16) Dorshow, R. B.; Bunton, C. A.; Nicoli, D. F. *J. Phys. Chem.* **1983**, *87*, 1409–1416.
- (17) Corti, M.; Degiorgio, V. *J. Phys. Chem.* **1981**, *85*, 711–717.
- (18) Ortega, F.; Bacaloglu, R.; McKenzie, D. C.; Bunton, C. A.; Nicoli, D. F. *J. Phys. Chem.* **1990**, *94*, 501–504.
- (19) Penfold, J.; Tucker, I.; Thomas, R. K.; Staples, E.; Schuermann, R. *J. Phys. Chem. B* **2005**, *109*, 10760–10770.
- (20) Shiloach, A.; Blankschtein, D. *Langmuir* **1998**, *14*, 7166–7182.
- (21) Puvvada, S.; Blankschtein, D. *J. Phys. Chem.* **1992**, *96*, 5567–5579.
- (22) Phillis, G. D. J.; Yambert, J. E. *Langmuir* **1996**, *12*, 3431–3436.
- (23) Carale, T. R.; Pham, Q. T.; Blankschtein, D. *Langmuir* **1994**, *10*, 109–121.
- (24) Tatiana, P.; Golub, T. P.; de Keizer, A. *Langmuir* **2004**, *20*, 9506–9512.
- (25) Heimenz, P. C. *Principles of Colloid and Surface Chemistry*; Marcel Dekker: New York, 1977.
- (26) Santhanalakshmi, J.; Goyal, P. S.; Aswal, V. K.; Vijayalakshmi, G. *Proc. Indian Acad. Sci. (Chem. Sci.)* **1999**, *111*, 651–658.
- (27) Varade, D.; Ushiyama, K.; Shrestha, L. K.; Aramaki, K. *J. Colloid Interface Sci.* **2007**, *312*, 489–497.
- (28) Prasad, Ch. D.; Singh, H. N.; Goyal, P. S.; Rao, K. S. *J. Colloid Interface Sci.* **1993**, *155*, 415–419.
- (29) Patil, R. R.; Guhagarkar, S. A.; Devarajan, P. V. *Crit. Rev. Ther. Drug Carrier Syst.* **2008**, *25*, 1–61.
- (30) Tian, Y.; Bromberg, L.; Lin, S. N.; Hatton, A. T.; Tam, C. K. *J. Controlled Release* **2007**, *121*, 137–145.
- (31) Lavasanifar, A.; Samuel, J.; Kwon, S. G. *Adv. Drug Delivery Rev.* **2002**, *54*, 169–190.
- (32) Yoo, H. S.; Park, T. G. *J. Controlled Release* **2001**, *70*, 63–70.
- (33) Jeong, B.; Bae, Y. H.; Lee, D. S.; Kim, S. W. *Nature* **1997**, *388*, 860–862.
- (34) Missirlis, D.; Kawamura, R.; Tirelli, N.; Hubbell, A. J. *Eur. J. Pharm. Sci.* **2006**, *29*, 120–129.
- (35) Bhattacharjee, J.; Verma, G.; Aswal, V. K.; Hassan, P. A. *Pramana* **2008**, *71*, 991–995.
- (36) Lo, Y. L.; Hsu, C. Y.; Huang, J. D. *Anticancer Res.* **1998**, *18*, 3005–3009.
- (37) Lo, Y. L.; Ho, C. T.; Tsai, F. L. *Eur. J. Pharm. Sci.* **2008**, *35*, 52–67.
- (38) van Hasselt, P. M.; Janssens, G. E. P. J.; Slot, T. K.; van der Ham, M.; Minderhoud, T. C.; Talelli, M.; Akkermans, L. M.; Rijcken, C. J. F.; van Nostrum, C. F. *J. Controlled Release* **2009**, *133*, 161–168.
- (39) Lasic, D. D. *Nature* **1992**, *355*, 279–280.
- (40) Lo, Y. L.; Huang, J. D. *Biochem. Pharmacol.* **2000**, *59*, 665–672.
- (41) Schuldes, H.; Dolder, J. H.; Zimmer, G.; Knobloch, J.; Bickeboller, R.; Jonas, D.; Woodcock, B. G. *Eur. J. Cancer* **2001**, *37*, 660–667.
- (42) Chae, H. W.; Kim, I. W.; Jin, H. E.; Kim, D. D.; Cheng, S. J.; Shim, C. K. *Arch. Pharm. Res.* **2008**, *31*, 103–110.

JP108225R